

Analysis of Strake-Slender-Wing Configurations Using Slender-Wing Theory

J. Krispin* and H. Portnoy†

Technion-Israel Institute of Technology, Haifa, Israel

A theoretical approach to investigating the flow over strake-slender-wing combinations is presented. The method developed consists of a modification of a well-known slender-wing-theory model together with the development of an approximate local solution in the kink region. This enables us to take care of the leading-edge discontinuity. The theoretical results predicted by the present method permit a rapid, qualitative investigation of the parameters that influence the vortex-flow patterns and the aerodynamic coefficients, within certain limitations and a comparison of configurations. Quantitatively, the calculation results in an overprediction of the forces. This trend is typical of slender-wing methods. The method could be readily extended to deal with the case of a strake-slender-wing arrangement mounted on a slender fuselage.

Introduction

THE model for a slender wing with leading-edge separation developed by Brown and Michael¹ for a delta wing and modified by Smith² to represent the separated flow past a slender wing with a curved leading edge is extended to treat strake-slender-wing combinations. The vorticity of the fluid near the strake leading edge, including the feeding sheet, is represented by a pair of isolated vortices of varying strengths. The kink in the leading edge introduces a disturbance that results in the formation of a wing leading-edge vortex. At the kinks, the feeding sheets of the strake vortices separate and their circulation remains constant thereafter.

Experimental support for this modeling is given by Luckring³ and Hoeijmakers and Vaatstra.⁴ An extensive qualitative discussion about the domain of validity of such modeling is given by Smith.⁵ Reddy⁶ investigated a double-delta wing using the sophisticated method developed by the Boeing Company⁷ in which the leading-edge vortex system is represented by free vortex sheets. The best agreement with experimental results was achieved while modeling two separate vortex systems on the inboard and outboard leading edges. A model based on two separate vortex systems has been applied in the present analysis, which, however, is much simpler than that of Ref. 7.

Mathematical Representation

Consider the inviscid, incompressible, irrotational, symmetric, steady flow of a uniform stream of velocity U at angle of attack α past a strake-slender-wing combination, as shown in Fig. 1. The basic assumptions made and the transformation applied to map the physical crossflow plane into the computational domain are those used by Smith.² Upstream of the kink, the equations are those of Smith.² Downstream of the kink, the introduction of the strake vortices above the plane of the wing (Fig. 2) leads to a system of four simultaneous differential equations:

$$2\pi U \sin \alpha = \Gamma_w \left(\frac{\bar{Z}_w^* + Z_w^*}{\bar{Z}_w^* Z_w^*} \right) + \Gamma_s \left(\frac{\bar{Z}_s^* + Z_s^*}{\bar{Z}_s^* Z_s^*} \right) \quad (1a)$$

$$U \cos \alpha \frac{d\bar{Z}_s}{dx} = \frac{\Gamma_w}{2\pi i} \left(\frac{Z_s}{Z_s^*} \right) \times \left\{ \frac{Z_w^* + \bar{Z}_w^*}{Z_w^* \bar{Z}_w^*} + \frac{1}{Z_s^* - Z_w^*} - \frac{1}{Z_s^* + \bar{Z}_w^*} \right\} + \frac{\Gamma_s}{2\pi i} \left(\frac{Z_s}{Z_s^*} \right) \left\{ \frac{Z_s^* + \bar{Z}_s^*}{Z_s^* \bar{Z}_s^*} - \frac{1}{Z_s^* + \bar{Z}_s^*} - \frac{s^2}{2Z_s^* Z_s^2} \right\} \quad (1b)$$

$$\frac{U \cos \alpha}{\Gamma_w} \left\{ (\bar{Z}_w - s) \frac{d\Gamma_w}{dx} + \Gamma_w \frac{d\bar{Z}_w}{dx} \right\} = \frac{\Gamma_w}{2\pi i} \left(\frac{Z_w}{Z_w^*} \right) \left\{ \frac{Z_w^* + \bar{Z}_w^*}{Z_w^* \bar{Z}_w^*} - \frac{1}{Z_w^* + \bar{Z}_w^*} - \frac{s^2}{2Z_w^* Z_w^2} \right\} + \frac{\Gamma_s}{2\pi i} \left(\frac{Z_w}{Z_w^*} \right) \left\{ \frac{Z_s^* + \bar{Z}_s^*}{Z_s^* \bar{Z}_s^*} + \frac{1}{Z_w^* - Z_s^*} - \frac{1}{Z_w^* + \bar{Z}_s^*} \right\} \quad (1c)$$

$$\frac{d\Gamma_s}{dx} = 0 \quad (1d)$$

where Γ is the vortex strength, Z the physical crossflow plane complex variable, s the local half-span, and Z^* the transformed plane complex variable, where $Z^{*2} = Z^2 - s^2$. Subscripts S and W refer to strake and wing vortices, respectively. Equation (1a) is a real equation that represents the fact that the Kutta condition is satisfied at the leading edge of the wing, i.e., a zero velocity at the transformed leading edge position assures a finite velocity at the physical leading edge.

The assumptions of Smith² along with the assumption that the strake vortices disconnect from the wing in the region of the kink and move downstream as free vortices lead to Eqs. (1b) and (1c). These are complex and describe the motion of the constant strength (strake) and varying strength (wing) vortices, respectively. Equation (1d) is a real equation that represents the constant strength of the free vortices.

A computer program is used to solve this set of differential equations for the six real unknowns: the strake and wing vortex strengths and the coordinates in the crossflow plane. While solving for the strake region, the calculation starts from an assumed conical flow near the strake apex, using the method of Brown and Michael¹ to find the initial position and strength of the pair of strake vortices. Marching downstream

Received Oct. 28, 1986; revision received May 26, 1987. Copyright © American Institute of Aeronautics and Astronautics, Inc., 1987. All rights reserved.

*Graduate Student; presently at Department of Aerospace Engineering, University of Maryland, College Park, MD.

†Adjunct Professor. Member AIAA.

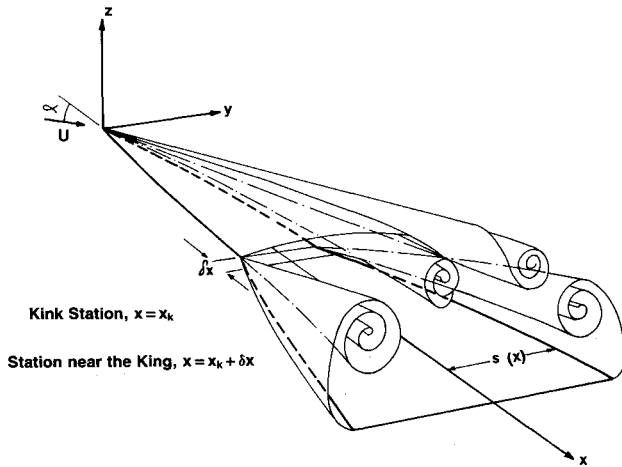


Fig. 1 Vortex system and notation.

towards the kinks, the equations used are those of Smith,² as previously mentioned. Here, the strake is actually treated as a slender wing with only one pair of vortices—the evolving strake vortices. To evaluate the kink vortex initial growth in the immediate vicinity of the kink, a first-order local solution is used. This, as expected, has nonconical features. The development of the approximate solution is presented in detail in the next section. Once the vortex strengths and coordinates are known, the lift coefficient and center of pressure can easily be determined using Sacks' law.⁸

Approximate Local Solution at the Kink Discontinuity

Consider two successive sections in the kink region, as shown in Fig. 1, $x = x_k$ and $x = x_k + \delta x$. We choose

$$\delta x/s_k \ll 1$$

where subscript k refers to the kink section. This choice, together with the physical behavior, yields

$$\begin{aligned} |\delta Z_S|/s_k &\ll 1 \\ |Z_W - s|/s_k &\ll 1 \\ (s - s_k)/s_k &\ll 1 \end{aligned}$$

At the section $x = x_k$, the wing vortices are still absent and the Kutta condition at the leading edge is satisfied by setting

$$2\pi U \sin \alpha = \Gamma_S \left(\frac{Z_{S_k}^* + \bar{Z}_{S_k}^*}{Z_{S_k}^* \bar{Z}_{S_k}^*} \right) \quad (2a)$$

where Z_{S_k} and $Z_{S_k}^*$ are, respectively, the values of Z_S and Z_S^* at $x = x_k$. At section $x = x_k + \delta x$, the Kutta condition is now satisfied by Eq. (1a) with appropriate values of Z_S and Z_S^* , i.e.,

$$\begin{aligned} 2\pi U \sin \alpha = \Gamma_S \left\{ \frac{Z_{S_k}^* + \delta Z_S^* + \bar{Z}_{S_k}^* + \delta \bar{Z}_S^*}{(Z_{S_k}^* + \delta Z_S^*)(\bar{Z}_{S_k}^* + \delta \bar{Z}_S^*)} \right\} \\ + \Gamma_W \left(\frac{Z_W^* + \bar{Z}_W^*}{Z_W^* \bar{Z}_W^*} \right) \end{aligned} \quad (2b)$$

Equation (2b) tends to the form of Eq. (2a) as $\delta x \rightarrow 0$, since $|\delta Z_S^*|$ and Γ_W also tend to zero.

Subtracting Eq. (2a) from Eq. (2b) and rearranging after

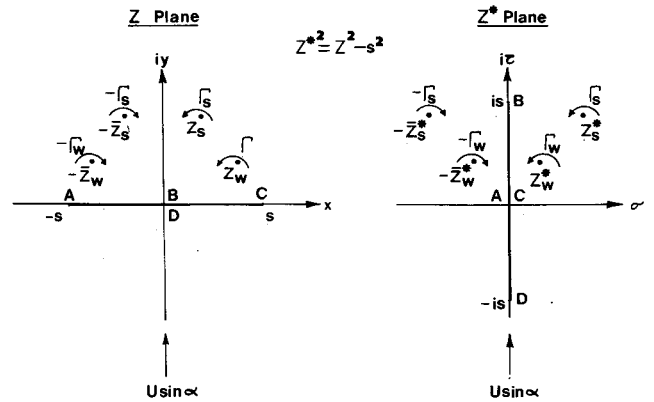


Fig. 2 Physical and transformed planes after the kink.

considering terms up to the first order yields

$$\Gamma_S \operatorname{Re} \left\{ \frac{Z_{S_k}}{(Z_{S_k}^2 - s_k^2)^{3/2}} \left(\frac{dZ_S}{dx} \right)_{x=x_k^+} \right\} \delta x \approx \Gamma_W \operatorname{Re} \left\{ \frac{1}{\sqrt{Z_W^2 - s^2}} \right\} \quad (3)$$

The terms forming the coefficient of δx on the left-hand side of Eq. (3) are independent of δx , so the first-order approximation to the right-hand side of Eq. (3) must also be of order δx .

The following power-law series are assumed:

$$\begin{aligned} \Gamma_W &= \gamma_W (\delta x)^n \left\{ 1 + \sum_{p=1}^{\infty} a_p (\delta x)^{q_p} \right\} \\ Z_W - s &= k_W (\delta x)^m \left\{ 1 + \sum_{p=1}^{\infty} b_p (\delta x)^{r_p} \right\} \end{aligned} \quad (4)$$

where r_p, q_p are general positive powers whose magnitudes increase with increasing p . Note that k_W and the b_p are complex numbers. Substituting Eq. (4) into Eq. (3) and rearranging, it is seen that the right-hand side of Eq. (3) becomes of order δx if $m = 2n - 2$. Equation (3), written to the first order, becomes

$$\gamma_W \operatorname{Re} \left\{ \frac{1}{\sqrt{2sk_W}} \right\} \approx \Gamma_S \operatorname{Re} \left\{ \frac{Z_{S_k}}{(Z_{S_k}^2 - s_k^2)^{3/2}} \left(\frac{dZ_S}{dx} \right)_{x=x_k^+} \right\} \quad (5)$$

The derivative is found from the conjugate of Eq. (1b) at $x = x_k$ (in which case the Γ_W terms vanish, $Z_S = Z_{S_k}$, etc.). Equation (4) requires $m > 0$ and thus $n > 1$.

Equation (5) involves two unknowns, k_W and γ_W . As an additional equation, Eq. (1c) is used. Substituting the power-law series description of the unknowns, Eq. (4), together with the already known relations $m = 2n - 2$, $n > 1$, into Eq. (1c) leads to

$$\begin{aligned} (3n - 2) U \cos \alpha \bar{k}_W (\delta x)^{2n-3} + U \cos \alpha \left(\frac{ds}{dx} \right)_{x=x_k^+} \\ = \frac{\gamma_W}{4\pi i} (\delta x)^{2-n} \left\{ \frac{1}{2k_W} + \frac{1}{\sqrt{k_W \bar{k}_W}} - \frac{1}{k_W + \sqrt{k_W \bar{k}_W}} \right\} \\ + \frac{\Gamma_S}{2\pi i s_k} \left\{ \frac{1}{\bar{Z}_S^2 - s_k^2} - \frac{1}{Z_S^2 - s_k^2} \right\} + O(\delta x^\ell), \quad \ell > 0 \end{aligned} \quad (6)$$

Equation (6) consists of two independent terms that do not involve the step size while in each one of the two other terms the step size can be eliminated by setting its power to zero, i.e., $n = 3/2$ or $n = 2$. If $n = 2$, the coefficient of γ_W is complex for general values of the argument of k_W while the other terms of the same order are real. Thus, n must be $3/2$. Applying this and solving gives a real value for k_W to first order. The power-law series then become

$$\begin{aligned}\Gamma_W &= \gamma_W \delta x^{3/2} + O(\delta x^i), & i > 3/2 \\ Z_W - s &= k_W \delta x + O(\delta x^j), & j > 1\end{aligned}\quad (7)$$

and Eq. (6), considering terms of up to the first order, becomes

$$\begin{aligned}\frac{5}{2} U k_W \cos \alpha + U \cos \alpha \left(\frac{ds}{dx} \right)_{x=x_k^+} \\ = \frac{\Gamma_S s_k}{2\pi i} \left(\frac{1}{Z_S^2 - s_k^2} - \frac{1}{Z_S^2 - s_k^2} \right) + O(\delta x^\ell), & \ell > 0\end{aligned}\quad (8)$$

One can evaluate k_W directly from Eq. (8). Knowing k_W , Eq. (5) is solved for γ_W .

Analysis of the Approximate Solution

Equation (8) shows that the position of the wing vortex k_W near the kink is the difference between two independent terms. The right-hand side of Eq. (8) is the complex velocity at the leading edge of the strake, just upstream of the kink. The second term on the left-hand side, $U \cos \alpha (ds/dx)_{x=x_k^+}$, depends upon the geometry of the wing. [The slope of the sweep angle of the wing just after the kink is $(ds/dx)_{x=x_k^+}$].

Since k_W is a real number (for first-order considerations), its magnitude describes the lateral distance between the wing vortex location and the wing leading edge [Eq. (4)]. For $k_W < 0$, the initial wing vortex lies above the wing surface, and its displacement above the wing is of the order of the neglected higher-order terms. It is difficult to accept such a solution from a physical point of view. Furthermore, we notice that Eq. (5), which is derived considering terms up to the first order only, gives an infinite value for γ_W for the case $k_W < 0$. Therefore, the region in which the approximate local

solution is valid is defined by

$$\frac{\Gamma_S s_k}{2\pi i} \left(\frac{1}{Z_S^2 - s_k^2} - \frac{1}{Z_S^2 - s_k^2} \right) \equiv (v)_{x=x_k} > U \cos \alpha \left(\frac{ds}{dx} \right)_{x=x_k^+}$$

where v is evaluated at the leading edge.

Peace⁹ presents a solution derived by Smith, which is similar to this analysis but more general and includes higher-order terms. His equations yield a solution which, again, seems physically implausible for $k_W < 0$.

Results and Discussion

A comparison between lift coefficients calculated using the present model and experimental results for several double-delta wings tested by Wentz and Kohlman¹⁰ shows a qualitative agreement (see Fig. 3). (Note that the double-delta wings calculated are slightly shorter than those tested due to the length limitation of the present method to be discussed later. Checking the effect of such small differences in length of the main wing for cases that could be calculated completely showed that they have negligible effect on the calculated normal force coefficient). Quantitatively, the present model overpredicts the forces. This is typical for a slender-body theory, in which the decrease in lift on approaching the trailing edge cannot be calculated, because the Kutta condition at the trailing edge is not fulfilled.

While calculating strake-slender-wing combinations, two limitations of the method were discovered. These are discussed in the next two sections.

Length (or Aspect Ratio) Limitation

While marching downstream, the strake free vortex tends to move toward the wing leading-edge vortex. If the wing is long enough in the chordwise direction, the two vortices come close together and the numerical scheme either breaks down or predicts enormous jumps in the locations of the vortices within a few successive integration steps. In a real flowfield, the wing vortex becomes dominant while advancing downstream, and it "swallows" or feeds on the strake-originated vorticity. The strake vortex vanishes or spreads its vorticity throughout large regions of the flowfield. More details are given by Hoeijmakers and Vaatstra⁴ and Smith.⁵

Such a situation cannot be simulated by the present model, since it assumes that the vorticity of each vortex is concentrated in its core and actually can be described as a point vortex in each section. Once the mathematical model is no

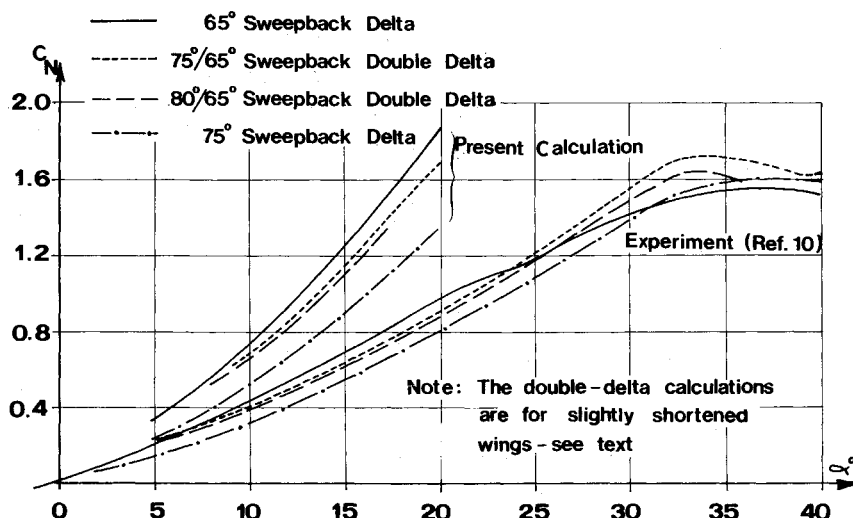


Fig. 3 Comparison between calculations and experiments for delta and double-delta wings.

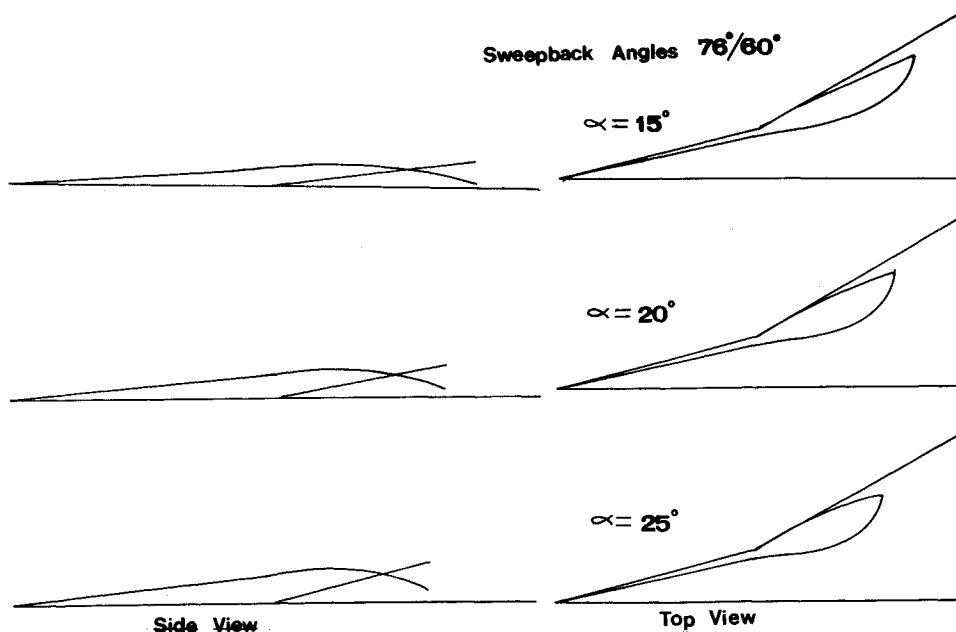


Fig. 4 Vortex trajectories above a double-delta wing at several angles of attack.

longer valid, there is no point in carrying on with the numerical calculations. Thus, the method is limited by the length (or aspect ratio) for which this difficulty first occurs.

The limiting length differs for each case and depends on the geometry of the configuration and the entire flowfield. It cannot be predicted a priori and is reached, if at all, while implementing the numerical solution. It was found that increasing the angle of attack decreased the distance along the x axis for which the difficulty first occurred. An example of this tendency is shown in Fig. 4. The trajectories of vortices above a double-delta wing at different angles of attack are described up to the point at which the numerical scheme breaks down. The flow patterns up to the breakdown nevertheless show a good qualitative agreement with the results obtained by Hoeijmakers and Vaatstra⁴ (c.f. Figs. 4 and 23 of Ref. 4).

Angle-of-Attack Limitation

The angle of attack strongly affects the domain of validity of the present method. For the approximate solution, the single mathematical condition that allows the initial growth of the kink (wing) vortices is

$$(v)_{x=x_k} > U \cos \alpha (ds/dx)_{x=x_k^+}$$

where v is evaluated at the leading edge.

Nevertheless, there are two independent physical cases for which these conditions are not satisfied.

1) When the angle of attack is small, the sidewash term is small. Thus, for a given $(ds/dx)_{x=x_k^+}$, there will be an angle of attack below which the local solution does not exist. It is reasonable to suppose that below this angle the strake-wing combination can be treated as one slender wing with varying angle of sweep and a single vortex system along the entire leading edge. This conclusion has been implemented in the calculations.

2) If the kink discontinuity is too large, $(ds/dx)_{x=x_k^+}$ will be large, and the local solution does not exist. Conditions do not allow the development of a wing vortex, even if the angles of attack are high. For this case, the flowfield is much more complicated and consists of both attached and separated flow regions. Such flowfields were experimentally investigated by Liu et al.¹¹ and many others.

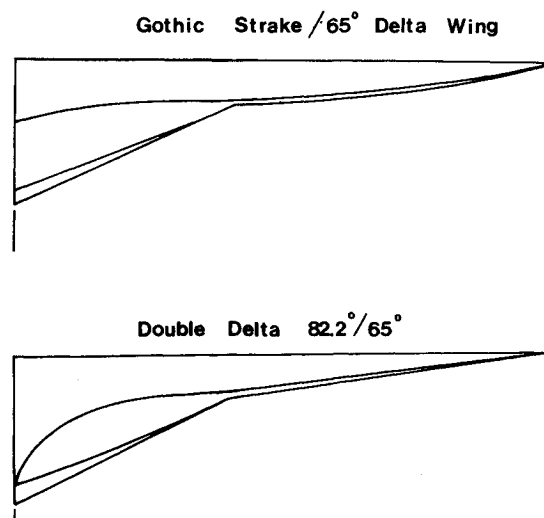


Fig. 5 Plan views of the vortex trajectories due to a delta strake and a gothic strake combined with a delta wing at $\alpha = 17.5$ deg.

Between the limiting low and high angles of attack, however, the model is valid and produces useful results.

Bloor and Evans¹² investigated the flowfield of a double-delta wing using a vortex discretization method. They found the same two limitations, i.e., kink size and wing length. In addition to those limitations arising from the condition for existence of a local solution, if the kink discontinuity is sufficiently small, the real physical flow may only be locally influenced by it, and the single-leading-edge-vortex model will be the correct one instead of ours, regardless of the mathematical existence of the local solution at the kink.

Interesting vortex flow patterns are shown in Fig. 5. In this case, the flowfield was calculated for two different types of strake combined with the same delta wing. For both combinations, the strake spans and lengths were kept the same, and the calculations were carried out for the same angle of attack. The difference between the two strakes was in the leading-edge curvature, one being a straight line (delta-type) and the other a curved, gothic type. From a comparison of the results, it is clear that although the vortex strengths do not differ much for

both cases (at the same locations along the x axis), the trajectories of the free vortices above the main wing are completely different. The vortices on the delta-strake-wing combination tend to be much closer together than those for the gothic-strake case.

An extensive parametric analysis showed that for low to moderate angles of attack, the addition of a strake did not improve the lift characteristics of the wing. Experimental studies by Wentz and Kohlman¹⁰ showed that the addition of a strake to a slender wing results in the vortex breakdown occurring at higher angles of attack than those for a wing without a strake. Thus, the benefits of such combinations are only felt at high angles of attack. The present model cannot calculate flowfields involving vortex breakdown. However, it enables comparisons to be made between different configurations at low and moderate angles of attack. Even though the numerical values of forces are overpredicted, the model provides a simple tool for better understanding of the flowfield and conducting rapid qualitative comparisons.

By use of a suitable conformal transformation, the method could be readily extended to deal with a strake-slender-wing system mounted on a slender fuselage. The effects of any nose vortices could also be included.

References

¹Brown, C.E. and Michael, W.H. Jr., "Effect of Leading-Edge Separation on the Lift of a Delta Wing," *Journal of Aeronautical*

Sciences, Vol. 21, No. 12, Dec. 1954, pp. 690-694 and 706.

²Smith, J.H.B., "A Theory of the Separated Flow from the Curved Leading Edge of a Slender Wing," British A.R.C., R&M 3116, 1959.

³Luckring, J.M., "Flow Visualization Studies of a General Research Fighter Model Employing a Strake-Wing Concept at Subsonic Speeds," NASA TM 80057, 979.

⁴Hoeijmakers, H.W.M. and Vaatstra, W., "On the Vortex Flow Over Delta and Double-Delta Wings," AIAA Paper 82-0949, 1982.

⁵Smith, J.H.B., "Theoretical Modelling of Three-Dimensional Vortex Flows in Aerodynamics," AGARD CPP 342, Article 17, 1983.

⁶Reddy, S.C., "Aerodynamic Performance of Slender Wings with Separated Flows," NASA-CR-168768, 1982.

⁷Johnson, F.T., Lu, P., Tinoco, E.N., and Epston, M.A., "An Improved Panel Method for the Solution of Three-Dimensional Leading-Edge Vortex Flows," NASA-CR-3278, Vol. 1, Theory Document, 1980.

⁸Sacks, A.H., "Vortex Interference on Slender Airplanes," NACA TN 3525, 1955.

⁹Peace, A.J., "A Multi-Vortex Model of Leading-Edge Vortex Flows," *International Journal for Numerical Methods in Fluids*, Vol. 3, 1983, pp. 543-565.

¹⁰Wentz, W.H. Jr. and Kohlman, D.L., "Wind-Tunnel Investigations of Vortex Breakdown on Slender Sharp-Edged Wings," University of Kansas Center for Research, Rept. FRL-68-013, 1968.

¹¹Liu, M.J., Lu, Z.Y., Qiu, C.H., Su, W.H., Gao, X.K., Deng, X.V., and Xiong, S.W., "Flow Patterns and Aerodynamic Characteristics of a Wing-Strake Configuration," *Journal of Aircraft*, Vol. 17, No. 5, May 1979, pp. 332-338.

¹²Bloor, M.I.G. and Evans, R.A., "Strake/Delta Wing Interactions at High Angles of Attack," JIAA TR-30, Stanford University, Stanford, CA, NASA-CR-166183, 1980.

From the AIAA Progress in Astronautics and Aeronautics Series

THERMOPHYSICS OF ATMOSPHERIC ENTRY—v. 82

Edited by T.E. Horton, The University of Mississippi

Thermophysics denotes a blend of the classical sciences of heat transfer, fluid mechanics, materials, and electromagnetic theory with the microphysical sciences of solid state, physical optics, and atomic and molecular dynamics. All of these sciences are involved and interconnected in the problem of entry into a planetary atmosphere at spaceflight speeds. At such high speeds, the adjacent atmospheric gas is not only compressed and heated to very high temperatures, but strongly reactive, highly radiative, and electronically conductive as well. At the same time, as a consequence of the intense surface heating, the temperature of the material of the entry vehicle is raised to a degree such that material ablation and chemical reaction become prominent. This volume deals with all of these processes, as they are viewed by the research and engineering community today, not only at the detailed physical and chemical level, but also at the system engineering and design level, for spacecraft intended for entry into the atmosphere of the earth and those of other planets. The twenty-two papers in this volume represent some of the most important recent advances in this field, contributed by highly qualified research scientists and engineers with intimate knowledge of current problems.

Published in 1982, 521 pp., 6 × 9, illus., \$29.95 Mem., \$59.95 List

TO ORDER WRITE: Publications Dept., AIAA, 370 L'Enfant Promenade, SW, Washington, DC 20024